

# Development of a coherent Doppler lidar for precision maneuvering and landing of space vehicles

Farzin Amzajerddian(a), Glenn D. Hines(a), Diego F. Pierrottet(b), Bruce W. Barnes(a), Aram Gragossian(b), Mitchell J. Davis(a), Tak-kwong Ng(a), Alexander D. Scammell(a), Adam Ben Shabat(a), Larry B. Petway(a), and John M. Carson III(c)

(a) NASA Langley Research Center

Hampton, Virginia 23693, USA

(b) Coherent Applications, Inc.

Hampton, Virginia 23693, USA

(c) NASA Johnson Space Center

Houston, Texas 77058, U.S.

**Abstract:** A coherent Doppler lidar has been developed to address NASA's need for a high-performance, compact, and cost-effective velocity and altitude sensor onboard its landing vehicles. Future robotic and manned missions to planetary bodies require precise ground-relative velocity vector and altitude data to execute complex descent maneuvers and safe, soft landing at a pre-designated site. This lidar sensor, referred to as a Navigation Doppler Lidar, meets the required performance of landing missions while complying with vehicle size, mass, and power constraints. Operating from over five kilometers altitude, the lidar obtains velocity and range precision measurements with 2 cm/sec and 2 meters, respectively, dominated by the vehicle motion. After a series of flight tests onboard helicopters and rocket-powered free-flyer vehicles, the Navigation Doppler Lidar is now being ruggedized for future missions to various destinations in the solar system.

**Keywords:** Coherent Lidar, Doppler Lidar, Precision Navigation, FMCW Lidar

## 1. Introduction

Global Positioning System (GPS) is commonly used in terrestrial navigation for vehicle position and velocity knowledge. In the absence of a GPS signal, past landing missions to planetary bodies primarily relied on radar to provide the necessary data to execute descent and landing maneuvers.<sup>1,2</sup> The Navigation Doppler Lidar (NDL) offers several critical advantages compared to radar, including significantly higher precision with reduced size, weight, and power. In addition, the laser-based NDL sensor does not suffer from measurement perturbation from terrain features or signal ambiguity from transmitted side lobes, and is far less susceptible to signal clutter, such as returns from the lander structure or jettisoned vehicle components such as heatshields. The higher quality data provided by the NDL will enable both a more precise navigation towards the designated landing site and a well-controlled touchdown (with greater stability and lower impact loads). This translates into lower fuel reserve and smaller leg span requirements for a landing vehicle which thus further reduces vehicle mass, therefore the NDL can potentially reduce the overall cost and risk of landing missions and enable new capabilities for planetary exploration missions including missions to the Moon, Mars, asteroids, and planetary moons.

## 2. NDL System Description

The principle of the lidar operation is illustrated in Fig. 1 which shows the modulation waveform consisting of three segments: up-ramp chirp, constant frequency, and down-ramp chirp. The resultant returned waveform from the target is delayed by  $t_d$ , the light round trip time. When the target or the lidar platform is not stationary during the beam round trip time, the signal frequency will be also shifted up or down, depending on the velocity direction, due to the Doppler effect. When mixing the two waveforms at the

detector, an interference signal is generated whose frequency is equal to the difference between the transmitted and received frequencies. In the absence of velocity along the laser beam, the signal frequency during the “up-ramp” and “down-ramp” periods are equal and their magnitude is directly proportional to the distance to the target. When the vehicle is moving, the up-ramp and down-ramp frequencies will not be equal and their difference is related to the Doppler velocity. The target range and magnitude of the velocity component along the laser beam are determined through the following simple equations:

$$R = \left( \frac{TC}{2B} \right) \left( \frac{f_{IF}^+ - f_{IF}^-}{2} \right) \quad V = \left( \frac{\lambda}{2} \right) \left( \frac{f_{IF}^+ + f_{IF}^-}{2} \right)$$

where  $f_{IF}^+$  and  $f_{IF}^-$  are the intermediate up-ramp and down-ramp frequencies,  $B$  is the modulation bandwidth,  $T$  is the waveform period,  $C$  is the speed of light, and  $\lambda$  is the laser wavelength. The constant frequency segment also produces a Doppler velocity that can be used for eliminating data dropouts when either up-ramp or down-ramp frequency is very close to zero, and allows for eliminating the measurement ambiguities that may arise in certain scenarios.

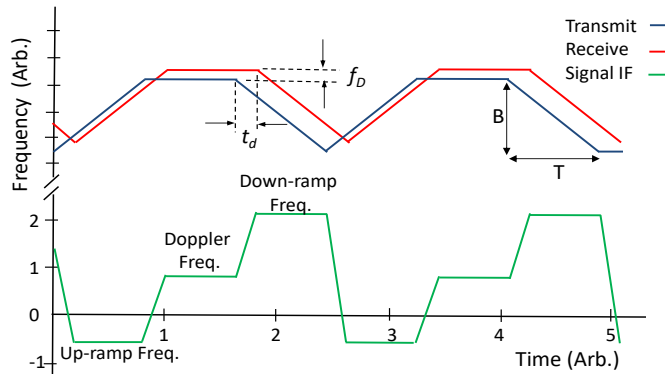


Figure 1. Linearly frequency modulated transmitted beam and returned signal, and the resulting intermediate frequency (IF) of the homodyne signal.

The NDL transmits three laser beams at different pointing angles toward the ground to measure range and velocity along each beam using a frequency modulated continuous wave (FMCW) technique.<sup>1</sup> The three line-of-sight measurements are then combined in order to determine the three components of the vehicle velocity vector and its altitude relative to the ground. Figure 2 shows the NDL prototype system developed for a series of flight tests to demonstrate its capabilities and viability for future landing missions to planetary bodies. The prototype consists of an electronic chassis and an optical head. All the lidar components including the transmitter laser, receivers, and signal processor are housed in the electronic chassis. The optical head consists of three transmit/receive lenses connected to the chassis via a fiber optic cable.



Figure 2. Prototype NDL.

### 3. Projected Performance

The NDL performance was characterized over different phases of its development through ground tests, helicopter flight tests, and onboard autonomous rocket-powered test vehicles (Fig. 3) while operating in open and closed-loop with a guidance, navigation, and control (GN&C) system.<sup>2,4</sup> The results of these tests helped optimize the NDL design leading to the development of a compact and robust prototype unit shown in Fig. 2.

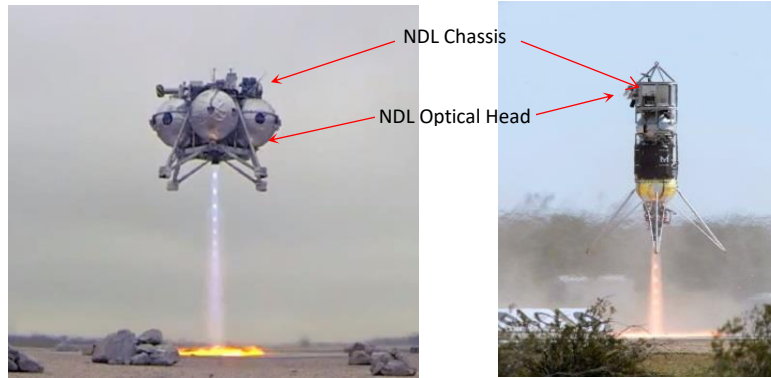


Figure 3. Morpheus vehicle (left), built by NASA-JSC, and Xodiac vehicle (right), built by Masten Space Systems, used for demonstration of NDL capabilities.

The NDL meets the performance requirements of almost all planetary landing missions being considered for launch over the next decade. The velocity precision and accuracy demonstrated in the flight tests are about an order of magnitude better than those required for well-controlled soft landing. The resolutions of line-of-sight (LOS) velocity and range measurements are 0.2 cm/sec and 25 cm, respectively, limited by the FFT processing algorithm. The NDL measurements precision, defined as random noise about its mean, was determined experimentally using flight test data. The LOS velocity and range precisions are about 1.7 cm/sec and 2.2 m, which were predominantly due to vehicle vibration and rapid angular motions. The NDL can measure velocities up to 200 m/sec along the LOS of its beams. The actual vehicle velocity can be significantly higher than 200 m/sec since there will always be an angular separation between the laser beams and the vehicle flight path. As a result, the NDL can measure vehicle velocities of well over 1000 km/hr.

The maximum operational range of the NDL is harder to define since it is highly dependent on the atmospheric environment and the surface albedo. To better assess the NDL performance in different terrestrial and planetary environments, a set of operational range measurements were performed on the Langley Air Force Base runway which provides a relatively long path length. For these tests, the NDL was placed at one end of the runway pointing one of its beams toward a calibrated target on the back of a moving box-car truck. The targets used for these measurements have a diffuse Lambertian surface and were placed nearly orthogonal to the NDL beam's optical axis. Range, velocity, and return signal magnitude data were collected continuously as the truck travelled from 250 meters range to 3.8 km.

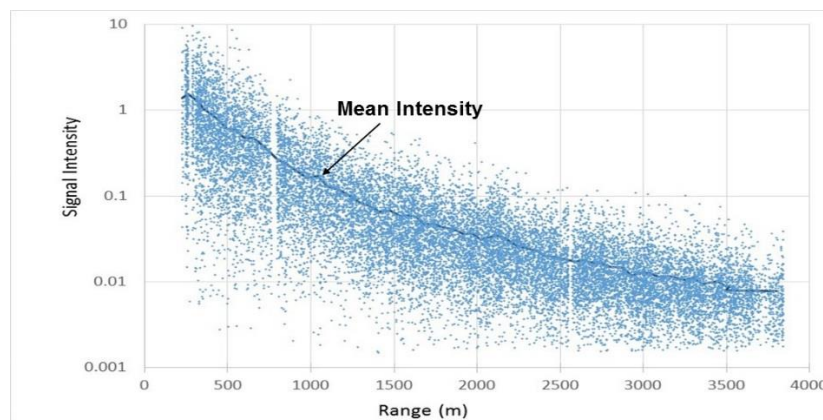


Figure 4. Signal intensity versus range.

Fig. 4 provides an example of signal intensity data as a function of LOS range using a 50 % reflectance target. The blue dots are the individual measurements, showing fluctuations due to speckle noise, and the solid line shows the mean of signal intensity data. Fig. 5 shows the lidar equation fit to measured data indicating a terrestrial maximum operational range of over 4 km in most atmospheric conditions and terrains. This is a conservative estimate considering that the measurements were performed over a horizontal path of approximately 1.5 m above the runway's concrete surface and in 70 % humidity. Using these results, the projected maximum LOS operational range on the Moon and Mars, under nominal atmospheric and surface albedo, were estimated to be 7.5 km and 5.7 km, respectively.

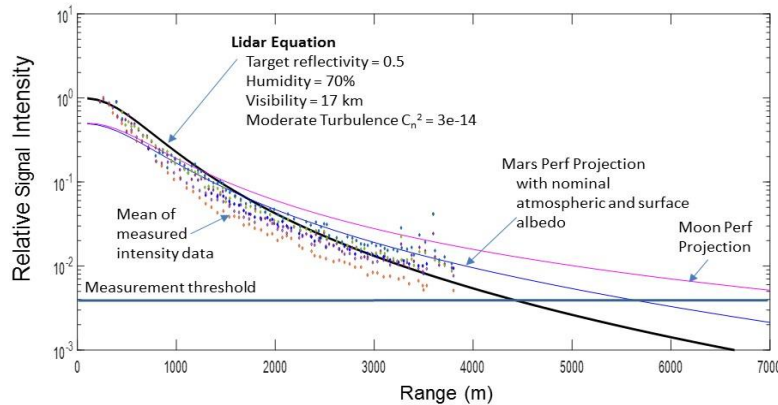


Figure 5. Estimated maximum operational range for operation on Earth, Moon, and Mars.

#### 4. Technology Advancement towards Spaceflights

The prototype lidar described above was designed with the vision of its eventual integration and operation from a planetary landing vehicle. The design of the prototype unit considered the size and mass constraints of landing vehicles and the harsh thermal and vacuum environments of space while meeting the performance requirements for a wide range of landing scenarios. This prototype unit is now serving as a testbed for the development of a spaceflight Engineering Test Unit (ETU) of the NDL intended to reduce the risk and cost of building spaceflight units. The ETU is being designed to meet the thermal, vacuum, and radiation environments of space and to be able to tolerate the launch vibration loads. Efforts are underway to build the components of the ETU using space-grade or spaceflight-qualifiable parts and validating their functionality, robustness, and reliability for operation in space. Once the ETU is fully assembled, it will be subjected to extensive spaceflight-qualification tests. The ETU will be then integrated with other landing vehicle avionics for a series of flight tests onboard aircraft and/or a rocket-powered free-flyer test vehicle prior to building the spaceflight units.

#### 5. References

- [1] F. Amzajerian, D. F. Pierrottet, G. D. Hines, L. B. Petway, B. W. Barnes, J. M. Carson III, "Development and Demonstration of Navigation Doppler Lidar for Future Landing Mission," AIAA Space Forum, 10.2514/6.2016-5590 (2016)
- [2] V. E. Roback, D. F. Pierrottet, F. Amzajerian, B. W. Barnes, G. D. Hines, L. B. Petway, P. F. Brewster, K. S. Kempton, and A. E. Bulyshev, "Lidar sensor performance in closed-loop flight testing of the Morpheus rocket-propelled lander to a lunar-like hazard field," Proc. of AIAA Science and Technology Forum and Exposition (2015)
- [3] Pollard, B. D., and Chen, C. W., "A Radar Terminal Descent Sensor for the Mars Science Laboratory Mission," IEEE Aerospace Conference, paper no.1597 (2008).
- [4] Pierrottet, D. F., Amzajerian, F., Petway, L. B., Hines, G. D., and Barnes, B. W., "Field Demonstration of a Precision Navigation Lidar System for Space Vehicles," AIAA GN&C Conference, 10.2514/6.2013-4717 (2013).